EARTHQUAKE ENGINEERING AND STRUCTURAL DYNAMICS
Earthquake Engng Struct. Dyn. 2005; **99**:1–26 *Prepared using* eqeauth.cls *[Version: 2002/11/11 v1.00]*

RC Pile-Soil Interaction Analysis using a 3D-Finite Element Method with Fiber Theory-based Beam Elements

T. Maki[1,*,†] , K. Maekawa[2] and H. Mutsuyoshi[1]

[1] *Department of Civil and Environmental Engineering, Saitama University*
255 Shimo-Okubo, Sakura-ku, Saitama City, Saitama 338-8570, Japan
[2] *Department of Civil Engineering, Graduate School of Engineering, The University of Tokyo*
7-3-1 Hongo, Bunkyo-ku, Tokyo 113-8656, Japan

SUMMARY

In order to develop a seismic response analysis method for examining RC structural systems, including foundations and the surrounding soil, we investigated the applicability of fiber theory-based beam elements to nonlinear simulations of laterally loaded RC piles. From the perspective of a subgrade soil reaction based on the one layer model, this paper discusses the appropriate modeling technique for pile-soil interaction analysis using beam elements, then proposes a basis for developing a guideline for modeling pile-soil systems. Applying the proposed models, numerical simulations were conducted using 3D-FEM for lateral loading test of RC piles. Also investigated was the influence of localized interfacial actions between the pile and the soil on the response behavior of pile-soil systems. The analytical model was verified quantitatively so that the proposed method can be used to evaluate actual structural seismic responses. Copyright © 2005 John Wiley & Sons, Ltd.

KEY WORDS: RC pile; interface between pile and soil; 3D-FEM; fiber model; beam element; response evaluation

1. INTRODUCTION

In the 1995 Hyogo-ken Nanbu earthquake, many RC structures, especially expressway and railway structures, suffered serious damage. Subsequent investigations proved the validity of the seismic design method, which is based on the ductility of yielded RC members. On the other hand, the pile foundations that supported the superstructures suffered relatively little damage during the earthquake, except that the foundations were exposed to the lateral flow of the surrounding soils.

Because there may have been damage to the non-strengthened members, such as the footings and piles, the seismic performance of RC structures, including members or structures that were strengthened after the earthquake, should be precisely evaluated. Evaluating the performance

*Correspondence to: Department of Civil and Environmental Engineering, Saitama University, 255 Shimo-Okubo, Sakura-ku, Saitama City, Saitama 338-8570, Japan
†E-mail: maki@post.saitama-u.ac.jp

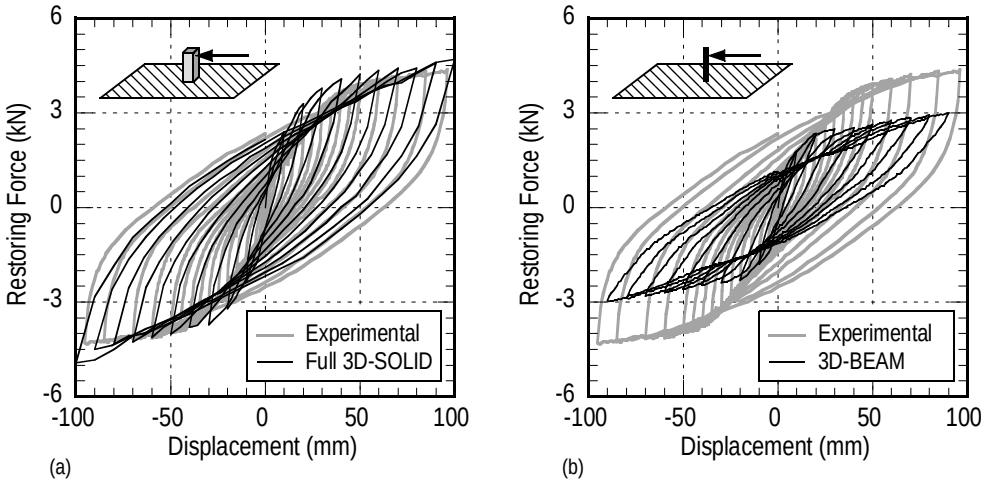

Figure 1. Load and displacement relationships of RC pile-soil system calculated by; (a) full-3D solid element model, and (b) 3D-beam element model.

of the overall structural system and improving the accuracy of the evaluation method are both urgent tasks. It is essential to develop a performance evaluation method based on the advanced analytical technologies that have been developed by various researchers and engineers.

From this perspective, response analysis using the finite element method (FEM) in the time domain, in which seismic motion is input to the engineering base, is an advanced technique for evaluating the overall response of structural systems is currently expected as such an advanced technique of the response evaluation method of overall structural system. This method automatically and explicitly includes the interactions between RC members or between a pile and its surrounding soil. The ability to obtain detailed damage information about the constitutive materials is another advantage of this method. The method is already a standard technique for evaluating the safety of important civil engineering structures such as nuclear power facilities [1]. It has also been prescribed in the JSCE standard specifications for concrete structures (seismic performance evaluation) revised in 2002 [2].

Since the 1995 earthquake in Japan, the seismic behavior of pile foundations subjected to large lateral cyclic deformations or high, fluctuating vertical loads has been widely examined [3, 4]. The authors have conducted several experimental and analytical investigations of the nonlinear behavior of RC pile-soil systems [5, 6, 7, 8]. However, detailed discussions of the applicability of FEM analysis to the seismic performance evaluation of pile-soil systems have only just started. In the framework of performance-based design, the safety margin in each limit state should be determined in relation to the accuracy of the evaluation technique. In other words, it is essential to completely verify the analytical method as well as improve the accuracy of the evaluation technique. Particularly in the case of seismic performance evaluation using FEM, it is necessary to verify not only the accuracy of the constitutive laws of the materials but also the appropriate combination of constitutive law and applied element type.

Figure 1 compares the lateral load and displacement relationships at the pile head. These

relationships were obtained from existing experiments and three-dimensional FEM analyses [7]. The hysteresis curve obtained from the analysis using full three-dimensional solid elements as a pile model agrees well with the results of the experiments, while the results obtained using beam elements had relatively low accuracy. Of course, a full-3D analysis is desirable when considering the three-dimensional effect of pile-soil interaction due to the volume of the pile. However, in the case of a large tank supported by thousands of piles, modeling all of the structural members using 3D solid elements does not have a reality with considering the calculation capacity of today's computers. Thus, there are still advantages to modeling piles using simple beam elements that have no volume.

This simplified reduction of the degree-of-freedom (dof) poses few problems when analyzing structures located above ground. However, when analyzing the interaction of a pile with the surrounding soil, the surface areas of the front, back, and both sides of the pile are ignored, resulting in an inappropriate evaluation of the soil pressures on the pile's surface. Therefore, the reproducibility of local deformation and the stress state of the soil that contacts the surface of the pile is inevitably inferior to that of an analysis using full three-dimensional solid elements. Consequently, the pile model should be complemented by additional modeling considerations when using the method for practical applications.

This paper discusses the application of a beam element model to RC pile-soil interaction analysis and the evaluation of the overall seismic responses of RC structure-foundation-soil systems using 3D FEM. In addition, based on the existing results of cyclic loading tests of RC piles under ground [8], the effect of localized interaction at the pile-soil interface on the response behavior of RC pile-soil systems is analyzed. Finally, the flexural and shear responses induced in the pile, including the effect of pile-soil interaction, are verified for a combined finite element model and nonlinear material model.

2. CYCLIC LOADING TEST OF RC PILES

Figure 2(a) shows the loading system in the experiment. The RC pile specimen was fixed to a rigid steel box, and the box was filled with dry sand that had grains of uniform diameter. The properties of the sand [9] are listed in Table I. Lateral reversed cyclic displacements were applied at the pile head through a loading actuator. Pile deformations and subgrade soil reactions were measured using strain gauges and earth pressure cells attached to the surface of the pile. The pile specimen was securely fixed to the bottom of a steel box to prevent rotation, while the pile head was allowed to rotate freely. The overall soil deformation was confined by the rigid soil box during loading. Although the conditions of the experiment were as close as possible to the actual conditions of the piles, some peculiar conditions were chosen to provide clear boundary conditions so that the results could be used in subsequent analyses.

In the experiment, the experimental parameters consisted of the cross sectional shape and longitudinal reinforcement ratio of the RC pile and the stiffness of soil. The soil stiffness was controlled by changing the relative density of the soil. Additional cases using two elastic piles were included in the program of experiments in order to verify the variations in the subgrade soil reactions on the surface of the pile. All of the experimental cases are summarized in Table II.

Figure 2(b) shows the cross sections of the specimens. All of the specimens had an equal projection width of 100 mm in the loading direction. Deformed bars having a diameter of 6

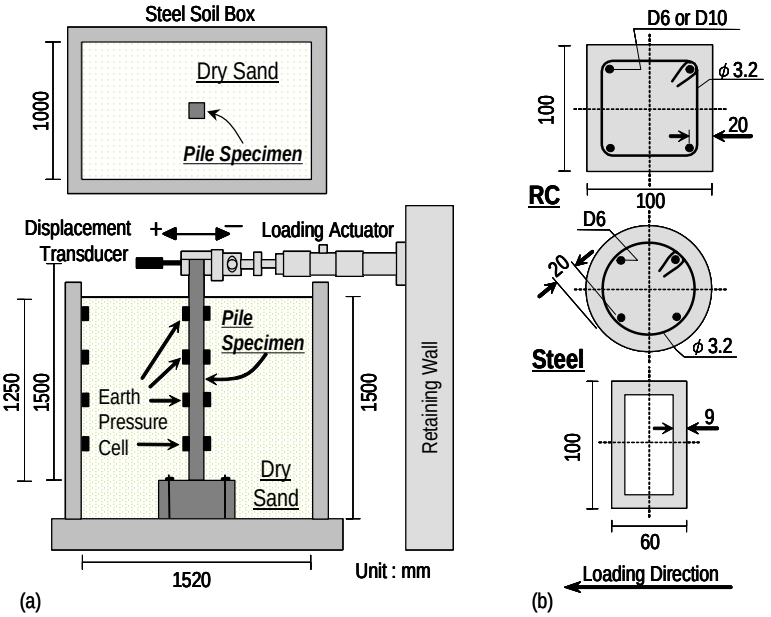

Figure 2. (a) Experimental loading system, and (b) cross sections of test specimens.

Table I. Properties of Gifu sand.

Specific Gravity	G_s	2.643
Maximum Diameter	$D_{max}(mm)$	0.84
60% Diameter	$D_{60}(mm)$	0.35
30% Diameter	$D_{30}(mm)$	0.31
10% Diameter	$D_{10}(mm)$	0.22
Uniformity Coefficient	U_c	1.59
Maximum Void Ratio	e_{max}	1.126
Minimum Void Ratio	e_{min}	0.717

mm or 10 mm were used as longitudinal reinforcements. Deformed bars having a diameter of 3.2 mm were arranged with 100 mm spacing as lateral reinforcements. The elastic steel pile specimen was a hollow rectangle cross section with an initial bending stiffness (EI) equal to that of the RC specimens.

The relative density of the soil was controlled by compacting the soil layer every 30cm thickness using a concrete block dropped onto the ground surface. The resulting relative density in each case is shown in Table II. The initial horizontal earth pressures were measured in all cases and the initial earth pressure coefficient, which is defined as a ratio of the horizontal to vertical pressures, ranged from 0.5 to 0.7 in the cases with loose soil, and from 2.3 to 4.0 in

Table II. Experimental variables of test cases.

No.	Case	Type	Section Shape*	f'_c (N/mm^2)	Long. Reinf.	Soil Cond.	Soil $D_r(\%)$	K_R $(\times 10^{-3})$
1	RCX-L	RC	Square	43.0	$\phi 10$	Loose	55.53	0.747
2	RCR-L	RC	Square	45.3	$\phi 6$	Loose	55.53	0.404
3	RCR-D	RC	Square	42.3	$\phi 6$	Dense	67.27	0.342
4	RCC-D	RC	Circle	44.3	$\phi 6$	Dense	71.28	0.203
5	STR-L	Steel	Hollow	——	——	Loose	55.53	1.497
6	STR-D	Steel	Hollow	——	——	Dense	73.49	1.212

the cases with dense soil. The relative pile-to-soil stiffness was calculated for each case using the above soil conditions and equation (1), which was proposed by Poulos [10]. The calculated K_R values are shown in Table II.

$$K_R = \frac{E_p I_p}{E_s L^4} \tag{1}$$

where, E_p is an elastic modulus of pile, I_p is an inertia moment of pile, E_s is an initial elastic modulus of the soil, and L is the embedded length of the pile.

Focusing on the force transfer mechanism between the pile and the soil, the results of these experiments were used to verify the proposed analytical method. Therefore, when applying the analytical method to actual structures, it is desirable to examine the measuring error and accuracy of the soil parameters, as well as the adequacy of the soil constitutive law as applied to the actual soil model.

3. SUBGRADE SOIL REACTIONS ON PILE SURFACE

3.1. Sectional force and subgrade soil reaction

When a structure supported by a pile foundation is exposed to ground motion at the engineering base, the piles are subjected not only to the inertial force of the superstructure but also to the soil pressures induced by ground deformation, as shown in Figure 3(a). In this case, the governing equation shown in the figure should be formulated, even if both the pile and the soil are nonlinear materials. In order to solve the differential equation shown in the figure, the nonlinearity of the soil is taken into consideration in the change in the subgrade soil reaction $q(z)$, and the pile's nonlinear events, such as cracking and yielding, are regarded as changes in the boundary conditions. Here, the subgrade soil reaction $q(z)$ is a resultant force, which acts on the pile at depth z. Therefore, to accurately calculate the sectional forces in a pile, the model must be able to appropriately evaluate the force transmitted between the pile and the soil.

As already shown in Figure 1, a *dof*-reduced model that uses beam elements underestimates the value, while a full- three-dimensional solid element model provides a finely traced result. In the case of a pile subjected at its head to a lateral force, the subgrade soil reaction distributed from the ground surface to the location of maximum moment governs the lateral load at the

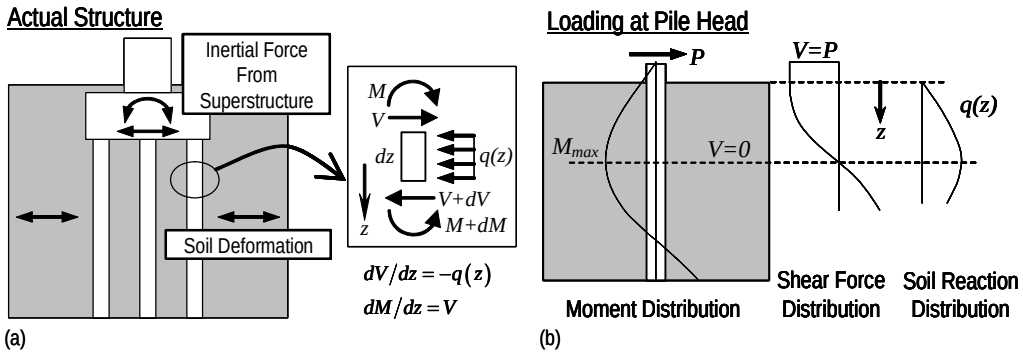

Figure 3. (a) Governing equations under earthquake, and (b) sectional force distributions of pile subjected to inertial lateral load.

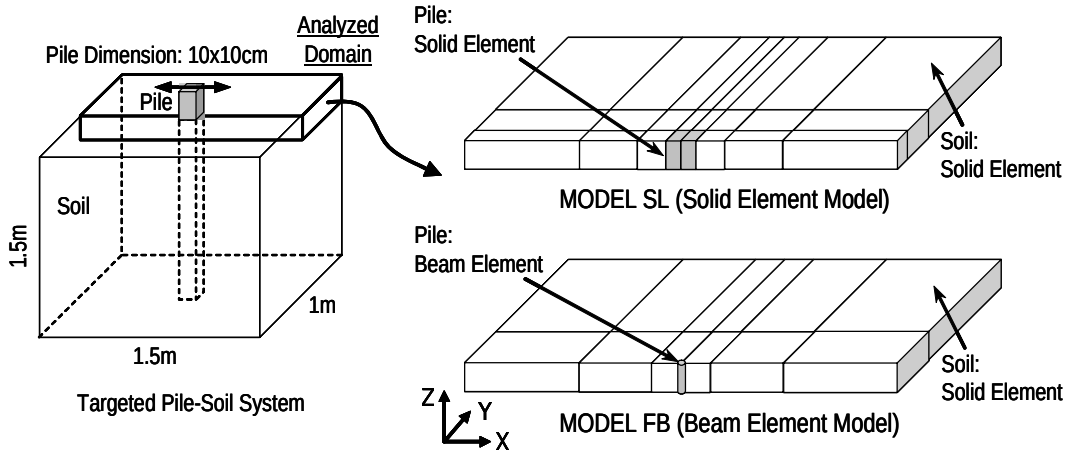

Figure 4. Basic 1-layer FEM model.

pile head, as illustrated in Figure 3(b). In this chapter, the influence of pile modeling on the release of the subgrade soil reaction is examined in detail [11].

3.2. Analytical Models and Parameters

Three-dimensional FEM code COM3 [12, 13] developed at the University of Tokyo was used in the analytical study. The basic finite element models are shown in Figure 4. Targeting the loading test of RC piles introduced in the previous chapter, a single-layer at ground surface was divided into several solid elements, each with 20 nodes, and solid elements or 3-node beam elements were used to model the pile. These two analytical models, Model SL and Model FB, were the basic models used in the analytical studies described in this chapter. In the pile-soil interaction analysis, the thickness of the soil layer should not be greater than the diameter of

Table III. Analytical parameters and cases.

Element Type	Case	Interface	Mesh Division	Gauss Integration
Solid	SL	no	——	2
	SL-J	yes	——	2
Beam	FB	no	coarse	2
	FB-J	yes	coarse	2
	FB-fine	no	fine	2
	FB-J-fine	yes	fine	2
	FB-g5	no	coarse	5
	FB-J-g5	yes	coarse	5

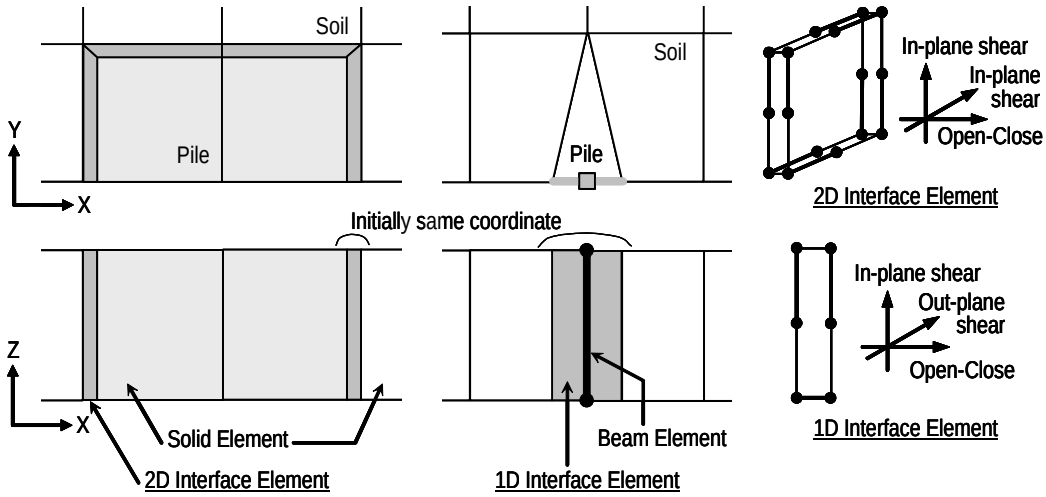

Figure 5. Profiles of interface element.

the pile. This is based on the idea that flexural deformation reappears in the pile. Therefore, the basic models had a thickness of 10 cm, which was equal to the diameter of the pile. Monotonic lateral displacement in the X direction was applied to all of the nodes of the pile elements.

The analytical parameters are shown in Table III. In addition to the element model of the pile, the presence of an interface element between the pile and the soil, the mesh division width around the pile, and the gauss integration order also were parameters in the analysis. The effect of the interface element was examined using both Model SL and Model FB, while the influences of the division width and the gauss integration order were studied using Model FB with and without the interface element. Here, the interface element takes into consideration the contact and the separation of the pile and the soil. A 16-node 2D interface element was applied to Model SL, and a 6-node 1D interface element was applied to Model FB, as shown in

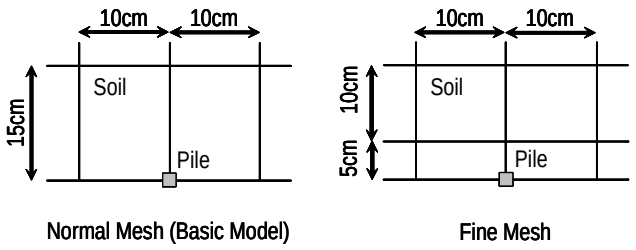

Figure 6. Mesh division width.

Figure 5. The 1D interface element was produced by condensing the dof of the Mindlin Plate element. Three nodes were connected to the beam element. The other nodes were connected to the soil solid element. Each node had three translational and three rotational dof, but the latter was ignored and all rotational components of the element stiffness matrix were null. In other words, the flexural moment induced in the beam element was not transmitted to the soil element. Therefore, only the normal stress and the in-plane and out-of-plane shear stress based on the three translational *dof*s were transmitted between the beam and the solid elements. Shear friction between the pile and the soil can be simulated using this interface element. In this paper, however, the 1D interface element, as well as the 2D interface element, were highly rigid in compression, while minute values were applied to the tensile and shear rigidities. In relation to the *dof* condensation of the element, it is necessary to incorporate the cross sectional area of the interface element, i.e., the contact area between pile and soil. In this paper, because the pile specimen has a square cross section, the contact area is the pile width multiplied by the element length.

The influence of the mesh division width was examined using the fine mesh model shown in Figure 6. The division width perpendicular to the loading direction was smaller in this model than in the basic model. The applied analytical code normally uses a gauss integration order of 2 for a 20-node solid element (reduced gauss integration). However, in Model FB-g5, a gauss integration order of 5 was adopted in order to examine the effects of localized stress transmission between the pile and the soil.

Both the solid element and the beam element used for the pile model were treated as elastic elements. For the soil material model, the Osaki model [14] expressed by the following equation (2) was adopted to define the relationship between the 2nd deviator invariant stress J_2 and strain J_2'.

$$\frac{J_2'}{M} = \frac{J_2}{2G_0M}\left\{1 + \left(\frac{G_0}{100S_u} - 1\right)\left|\frac{J_2}{S_uM}\right|^B\right\} \tag{2}$$

where, G_0 is the initial shear modulus, S_u is the shear strength at 1% shear strain, B is the material parameter (1.6 for sand and 1.4 for clay), and M is the loading parameter (1.0 when loading, and 2.0 when unloading or reloading).

This model is already verified up to 1% shear strain level based on the stratified soil response. The average (volumetric) stress-strain relationship is assumed linear elastic, and tensile stress is allowed. The volumetric elasticity is calculated from the initial shear modulus and Poisson's ratio (a constant value of 0.3 in this analysis) based on the elasticity theory. In this material

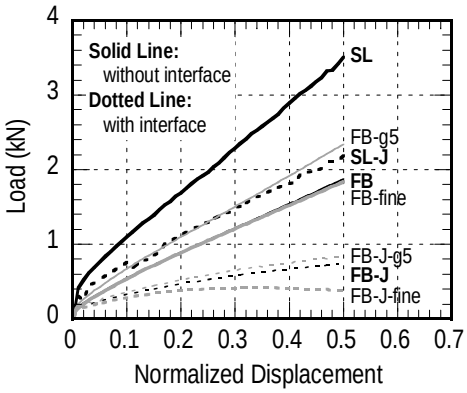

Figure 7. Load-displacement relationships.

model, the effect of confinement (volumetric stress state) on the shear modulus and strength was ignored. The soil used in the analytical model was sand with an initial shear modulus $G_0 = 19.6N/mm^2$ and a shear strength at 1% shear strain $S_u = 0.00294N/mm^2$, as determined from the conditions of the experiment.

3.3. Analytical results

Figure 7 shows the relationships between the lateral load and the displacement for all of the models. Here, the lateral load is a summation of the reactions at all of the loading nodes, and lateral displacement δ is expressed with a dimensionless value normalized by the pile diameter D (= 100 mm). Model FB had half of the lateral load of Model SL. Furthermore, the lateral load lost in the model with an interface element was about half that of Model FB and a third that of Model SL. This decrease in lateral load for the model with an interface element was due to the elimination of tensile stress at the back of the pile body. The details are described later in this chapter.

The influence of the mesh division width around the pile was barely seen in the model without an interface element. On the other hand, the mesh division width had a very significant effect in the model with interface element. The soil elements in front of the pile element were subjected to a linear load when the pile was modeled by a beam element. Therefore, in Model FB-J-fine, localized plasticity increased in the soil element, which resulted in a ceiling on the lateral load.

A slightly higher lateral load was observed in the model with a gauss integration order of 5, even at the same mesh division. This is because, in the model with a gauss integration order of 5, the gauss point coordinate approached that of the pile element so that the localized stress at gauss point is sensitively reflected in the subgrade reaction rather than in the basic model. The results of the analysis of Model FB-g5, as shown in Figure 7, are very close to that of Model SL-J.

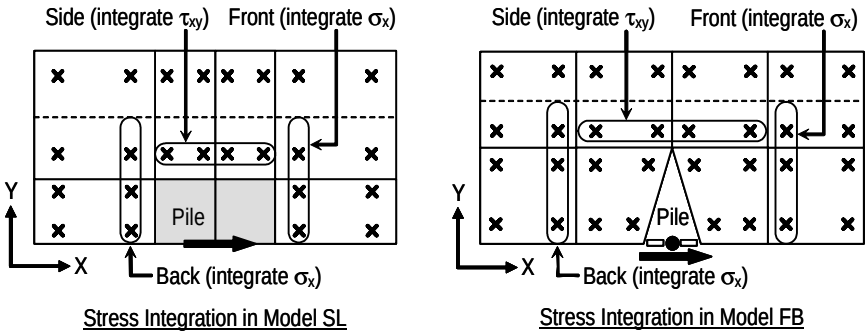

Figure 8. Schematic concept of stress integration.

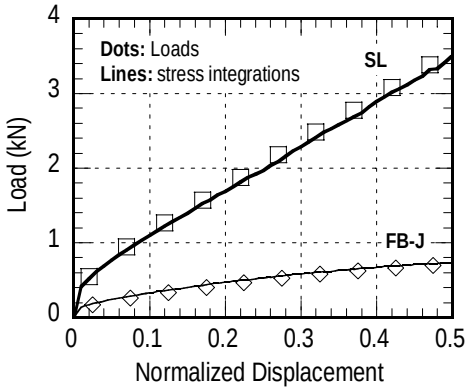

Figure 9. Results of stress integration.

3.4. Decomposition of subgrade soil reaction around the pile

In the previous section, the total lateral load was regarded as a subgrade soil reaction on the pile, while the actual pile was subjected to a soil reaction on the front, back, and sides. Therefore, the total subgrade reaction discussed in the previous section was a summation of the reactions at surfaces normal to all directions. Here, the total subgrade reaction is decomposed into three types of reactions on the front, back and side surfaces of the pile by integrating the soil stress values at the gauss points around the pile. Figure 8 shows the schematic concept of the decomposition of the subgrade reaction in both the SL-type and FB-type models. In the SL-type models, the normal or shear stresses at all of the gauss points around the pile element are used for stress integration, while in the FB-type models, the stress values at the gauss points around the soil elements next to the pile element are integrated. Examples of the stress integration results for Model SL and Model FB-J are shown in Figure 9, while the stress integration values in all eight of the cases that coincided with the lateral loads are shown in Figure 7. The above-mentioned stress integrating scheme is the subject of the following

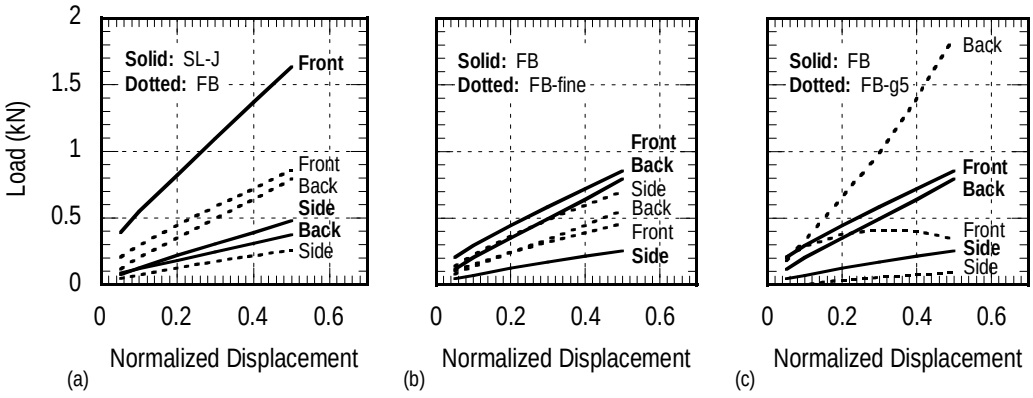

Figure 10. Comparisons between subgrade reaction shares in; (a) SL-J and FB, (b) FB and FB-fine, and (c) FB and FB-g5.

discussion of the distribution of the subgrade reaction around the pile.

3.5. Subgrade reaction distribution around pile

Figure 10(a) shows the integrated results of the reactions on the front, back, and side surfaces of the piles in Model SL-J and Model FB. The total subgrade reactions in these two models are almost equal, as shown in Figure 7. In Model SL-J, the reaction on the back surface is very low due to the introduction of the interface element, while the reaction on the front surface is high. On the other hand, similar values for the reactions can be observed on the front and back surfaces in Model FB. Considering that, among all the examined models, Model SL-J most closely models actual pile conditions, these results indicate that the total subgrade reaction approaches that in Model SL-J. This is because tensile stress is allowed to occur in the soil material model, although the reaction at the front surface in Model FB is underestimated because of the use of beam elements for the piles.

Figure 10(b) shows the similar results that were obtained from Models FB and FB-fine. In addition, the total subgrade reaction in Model FB-J was equal to that in Model FB, as shown in Figure 7; however, the distribution of the subgrade reactions in these models was completely different. The front and back reactions in Model FB-fine were lower than those in Model FB and the side reactions accounted for the differences in the reactions at the front and back surfaces.

Figure 11 shows the normal stress distributions in the soil at the front surfaces of Model SL-J, FB, and FB-fine. The stress distribution in Model FB is more similar to that in Model SL-J than to that in Model FB-fine. Therefore, if beam elements are used for the pile models, then a realistic soil stress state can be obtained by using a comparatively coarse mesh division (about three times as large as the pile dimension in Model FB). Taking into consideration the applied soil material model and the above-mentioned results, almost the same degree of total subgrade reaction can be derived from the model that uses beam elements for the piles by allowing tensile stress in the soil and using a relatively coarse soil mesh division.

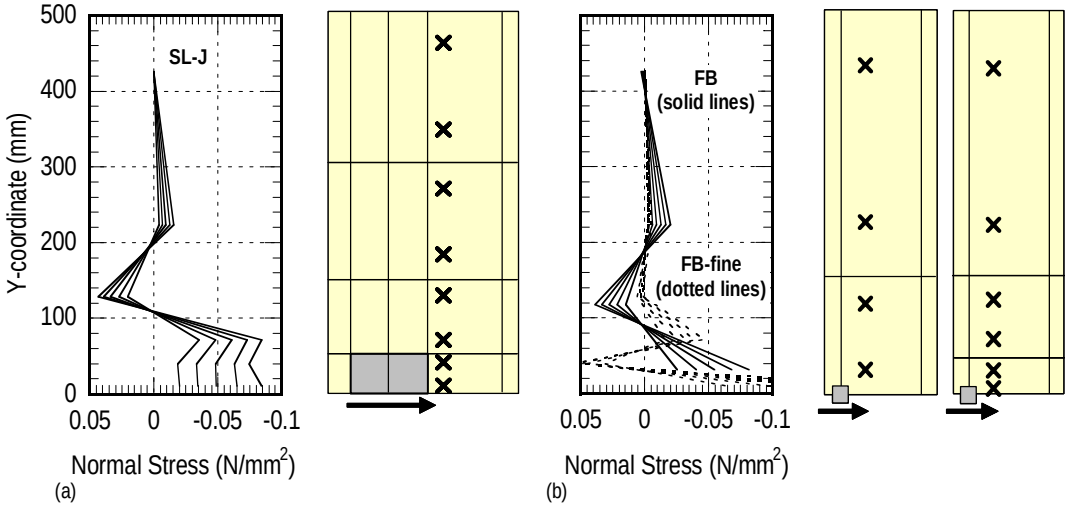

Figure 11. Normal stress distributions in; (a) Model SL-J, and (b) Model FB and FB-fine.

Figure 10(c) shows the results for Models FB and FB-g5. This figure shows that the difference in the total subgrade reactions in these models (as shown in Figure 7) derives from the excess increase in tensile force at the back surface in Model FB-g5. The softening behavior of the front-surface reaction in Model FB-g5 comes from localized plasticity due to the linear localized load exerted by the pile. These reactions at the front and back surfaces are not realistic even though they are similar to the total subgrade reaction in Model SL-J.

3.6. Summary

This chapter discussed the influence of the pile model on the subgrade soil reaction. When a pile is modeled using a beam element without volume, the decomposed reaction on the front surface is underestimated. However, if soil tensile stress is allowed and no interface element is introduced between the pile and the soil, the total subgrade reaction in such a model is almost equal to that observed in a model that uses solid elements for the pile. If an interface element with no tensile stiffness is used, it is important to keep in mind the possibility of underestimating the total subgrade soil reaction. Moreover, using a relatively coarse mesh division for the soil around the pile appropriately distributes the stress in the soil.

4. PILE-SOIL INTERACTION ANALYSIS

4.1. Analytical model and constitutive laws of reinforced concrete

Figure 12(a) shows the finite element mesh used for loading test simulations of the soil-pile systems described in the second chapter. The pile specimen was modeled using 3-node RC

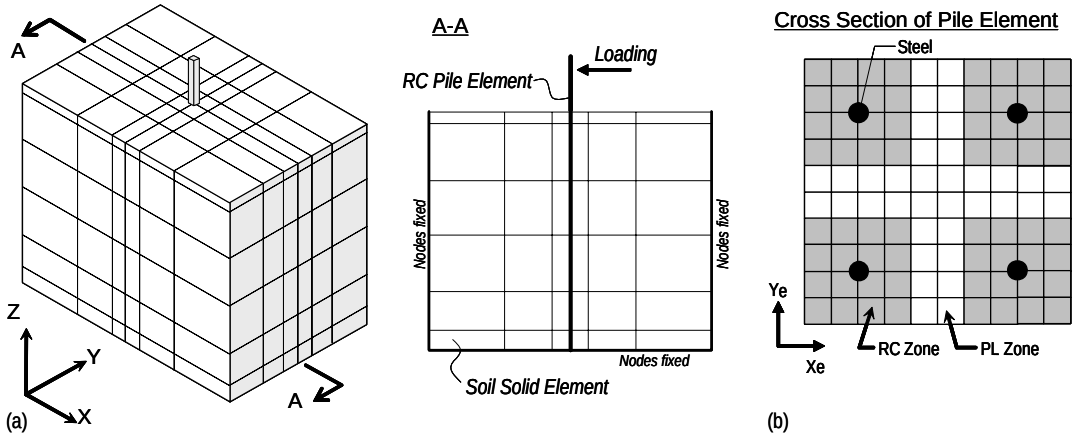

Figure 12. (a) Finite element modeling of pile-soil system, and (b) cross section of pile element.

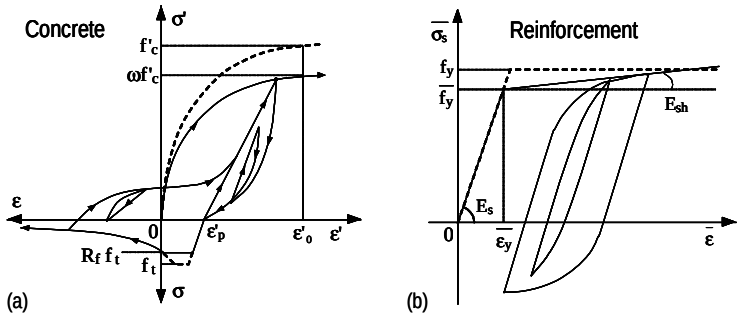

Figure 13. Constitutive laws of (a) concrete, and (b) reinforcement.

beam elements based on a fiber model [13]. In these elements, the axial force and the flexural moments are calculated using the averaged axial strain and two directional curvatures. In the calculation, the cross section of the element is divided into minute cells (fibers), as shown in Figure 12(b), in relation to the longitudinal reinforcement arrangement. The uniaxial stress-strain relationships of the concrete and the reinforcement, illustrated in Figure 13, are applied to each cell [13]. These constitutive laws were obtained by modifying the existing three-dimensional constitutive laws for reinforced concrete [12]. Additionally, a zoning technique [15] was used for modeling the cross section, as shown in Figure 12(b). The RC zone is an area of effective tension stiffening of the longitudinal reinforcement, resulting that the tension stiffening parameter c in the tensile stress-strain curve of concrete is a constant value of 0.4, while in the PL zone, the c parameter is dependent on the element size and the fracture energy of plain concrete. The shear formulation of the element is assumed linear elastic. The constitutive law of the soil is the same as for the model described in the previous chapter.

As shown in Figure 1, the soil stress state around the pile is remarkably effective at predicting the pile-soil interaction. The finite element mesh shown in Figure 12(a) is constructed based

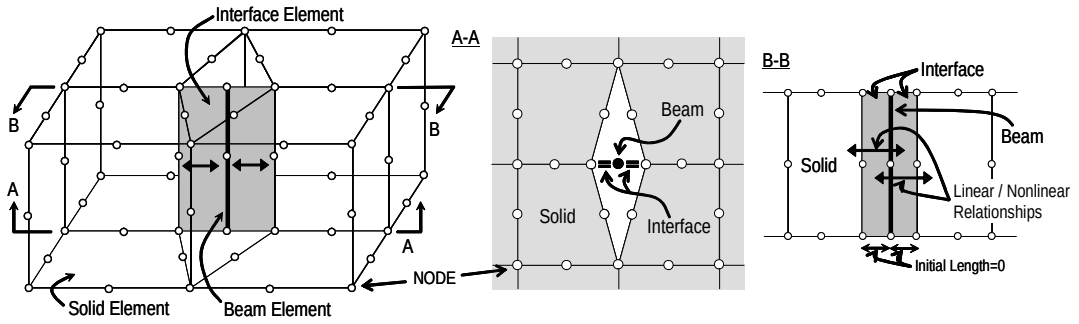

Figure 14. Interface element between pile and soil.

on the investigations in the previous chapter. These analytical treatments were intended to simulate the equivalent stress state of real soil around real piles, and therefore should be used only for *dof*-reduced analysis, as well as the interface element introduced at the wall-column interface of seismic resistant walls to consider the three dimensional interaction by using dimension-reduced 2D analysis [12].

Figure 14 shows the specifications of the interface element introduced at the pile-soil boundary. It is similar to that of the model described in the previous chapter. The contact area of the element is defined by the pile width multiplied by the element length. However, when simulating the behavior of a circular pile, the effective contact area between the pile and the soil should be considered. Further investigation is needed to define the effective area. Moreover, in Figure 14, the interface elements are arranged only in one direction because the applied load in the targeted experiment was unidirectional. However, actual pile foundations are subjected to bidirectional loading or vibration. Therefore, additional investigations of the element arrangement and contact area setting are needed to make the model practically applicable to bidirectional behaviors.

The previous chapter discussed only the influence of the tensile force at the back surface of the pile. However, the pile-soil cyclic interaction that will be investigated in this chapter, especially the localized behavior at the pile-soil interface, is affected by the earth pressure distribution in the Z direction and by sand consolidation resulting from pile deformation, as shown in Figure 15. These effects have already been described by the authors in a previous paper on pile-soil behavior [6]. That paper considered four types of linear/nonlinear interface characteristics, which are illustrated in Figure 16 of this paper. Here, Model EL is a perfect elastic model and Model NT is the no-tension model used in the previous chapter. Model EP is a no-tension model that considers the initial earth pressure distributions in the Z direction, and Model EPC includes the effect of sand consolidation due to cyclic deformation of the pile. Based on these previous results, sand consolidation had little influence on the pile behavior. This paper discusses the effects of the tensile force and the earth pressures, focusing on Model EL and Model EP. The shear friction at the interface is ignored in this analytical investigation.

Model EL is a perfect elastic model in which the normal stress-strain relationship is assumed linear elastic and the stiffness is high normal, as shown in Figure 16(a). Using this model, the nodes of the pile and the soil element move with perfect consistency, as they do in the analytical

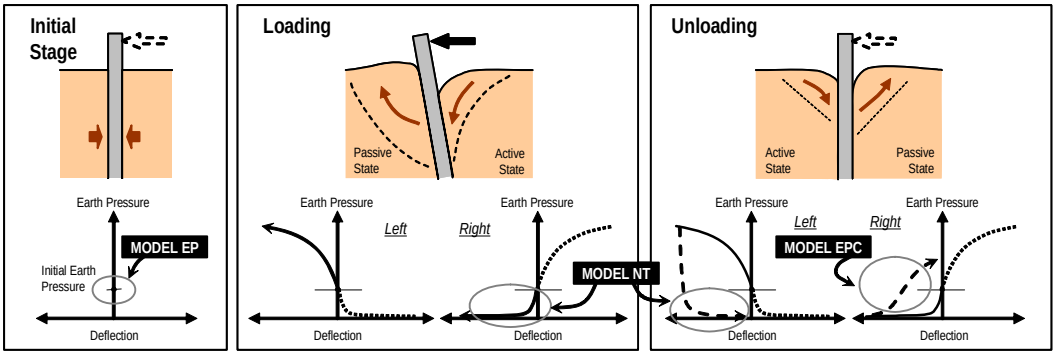

Figure 15. Interfacial behavior idealization of soil around pile.

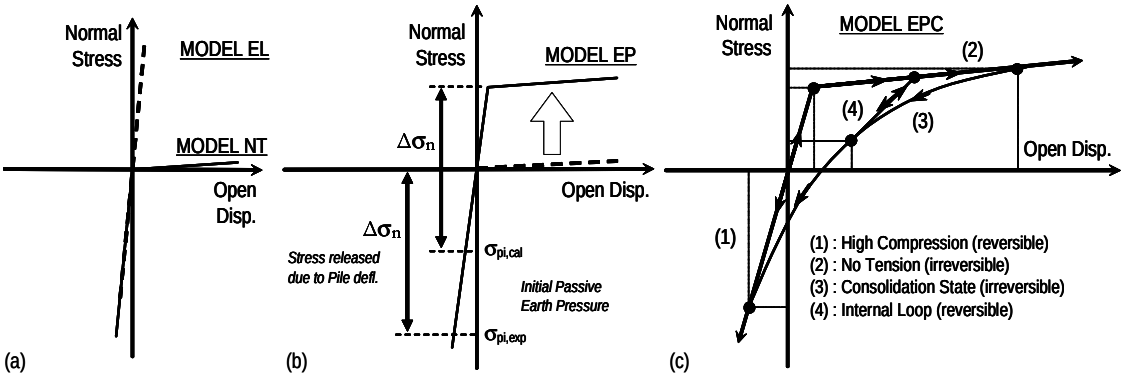

Figure 16. Linear and nonlinear constitutive laws of interface element; (a) Model EL and NT, (b) Model EP, and (c) Model EPC.

model without an interface element. Model EP is a no-tension model that incorporates the initial earth pressures. In the targeted experiment, the model soil was dry sand with no tensile stiffness. Therefore, almost no soil pressure acted on the back surface of the pile (no active soil pressure), as shown in the center drawing of Figure 15. Such behavior is taken into consideration by this model, in which the high stiffness is activated only on the compression side in order to avoid generating tensile stress at the pile-soil interface (no tension). In actual behavior, when the stress state at the interface shifts from compression to tension, *separation* occurs. In the targeted experiment, the soil stiffness was controlled by manually dropping a concrete block onto the surface of the ground in order to create sand with a high relative density. This resulted in an excessively passive initial stress state in the modelled soil. The measured initial earth pressure coefficient K_p within the embedded length of the pile ranged from 2.3 to 4.0, and these high passive earth pressures on the pile surface were released due to lateral loading during pile deformation. Compared to the the initial horizontal earth pressure coefficient in the experiment, the initial horizontal earth pressure coefficient in the analysis was around 0.4

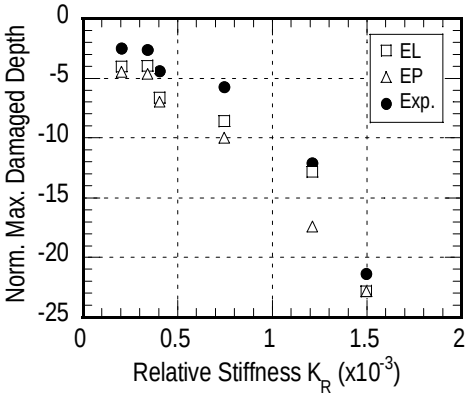

Figure 17. Variations of maximum damaged depth.

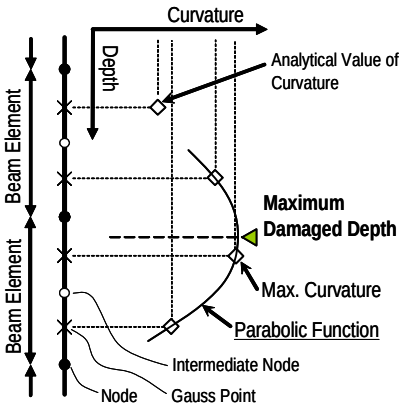

Figure 18. Determination of maximum damaged depth.

because the analysis used a very simple constitutive law of soil, such as a hyperbolic type shear stress-shear strain nonlinear relationship that is independent of the average stress state, and the Poisson's ratio was kept constant at all possible strain levels. Therefore, in Model EP, the yield point shifted towards the tension side so that the stress difference released during pile deformation coincided with the initial earth pressure measured in the experiment, as illustrated in Figure 16(b). As stated in the previous chapter, the interface element described in this paper does not transmit the induced flexural moment in the beam element to the soil element. However, the actual pile behavior under ground is governed by the flexural deformation of the pile itself. Therefore, the investigation in the previous chapter is inadequate. Further investigation of the flexural and shear behavior of the piles in the pile-soil interaction analysis is required.

4.2. Influence of interfacial behavior on response of RC piles

The depth from ground surface, where the widest crack is observed, is defined as the representative parameter of pile deformation under ground. This is called *the maximum damaged depth* in this paper and is denoted by L_{max} in the following figures. The maximum damaged depth is almost same as the maximum moment depth. Figure 17 shows the experimentally and analytically obtained variations in the maximum damaged depth of a pile with a relative stiffness of K_R, as shown in Table II. Here, L_{max} is normalized by the pile diameter D. The maximum damaged depth obtained from the calculation is determined from the curvature values at the gauss points of the beam elements, as illustrated in Figure 18. Accordingly, three curvature values, including the maximum curvature, is interpolated by the quadratic function of the gauss point coordinate, and the coordinate of the top of the quadratic curve is defined in the analysis as the maximum damaged depth.

From the experimental results, the maximum damaged depth linearly changes under different K_R values. This tendency can be simulated by the adopted analytical method. However, the analysis overestimates the maximum damaged depth as compared to that estimated by the experiment, particularly the analytical cases that considered the separation at the pile-soil interface. The maximum damaged depth itself does not affect on the seismic performance evaluation of structures supported by pile foundations. However, the error in the estimated maximum damaged depth is least effective in the restoring force evaluation at the pile head, based on the mechanism of force transmission between the pile and the soil that has already been reported in a previous paper [16].

The representative skeleton curves of the lateral load and displacement relationships in steel piles and RC piles are illustrated in Figure 19. These skeleton curves are drawn by connecting the plotted points for the maximum displacement in each repetition of the obtained hysteresis curves. The accuracy of the lateral load estimation is very high at low displacement levels, but the lateral load is underestimated in analyses that consider the separation at the pile-soil interface. This underestimation is due to modeling the piles using beam elements without volume, because the soil reaction on the front surface of the pile in the loading direction is underestimated in the model's beam elements, as discussed in the previous chapter. However, in the analysis of Model EL, which used interface elements with a high normal stiffness in both tension and compression, tensile stress occurred between the pile and the soil at the back surface of the pile. Therefore, in the case of Model EL, the lateral load at the pile head is the sum of the underestimated soil reaction in the front and the tensile force at the back, and consequently the results of the analysis and the experiment agree. However, in cases using Model EP with interface elements in which the tensile force is ignored, only the underestimated soil reaction is reflected in the lateral load at the pile head, resulting in the large difference in the lateral load values of the experimental and the analysis. Detailed modeling of the force transmitted at the pile-soil interface reveals the shortcomings of using beam elements in the pile model. The compressive and tensile soil reactions discussed above are sensitive to the element division of the soil around the pile. Those discussions are very similar to those in the previous chapter.

The variations in the equivalent damping coefficient are shown in Figure 20. They are the representative factor in the shape and area of the inner hysteresis loops of the lateral load and displacement relationships. The results of the analysis are lower than the results of the experiment, with a maximum difference in the damping ratio of about 10%. The effect of

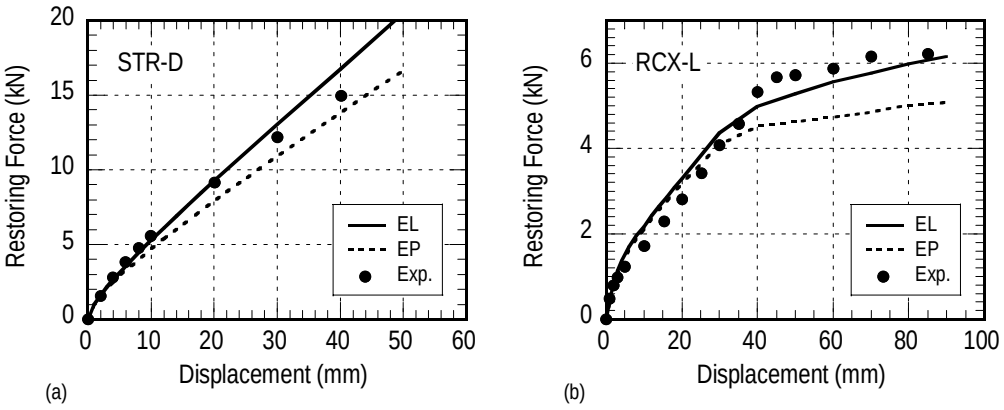

Figure 19. Load-displacement skeleton curves in (a) STR-D, and (b) RCX-L.

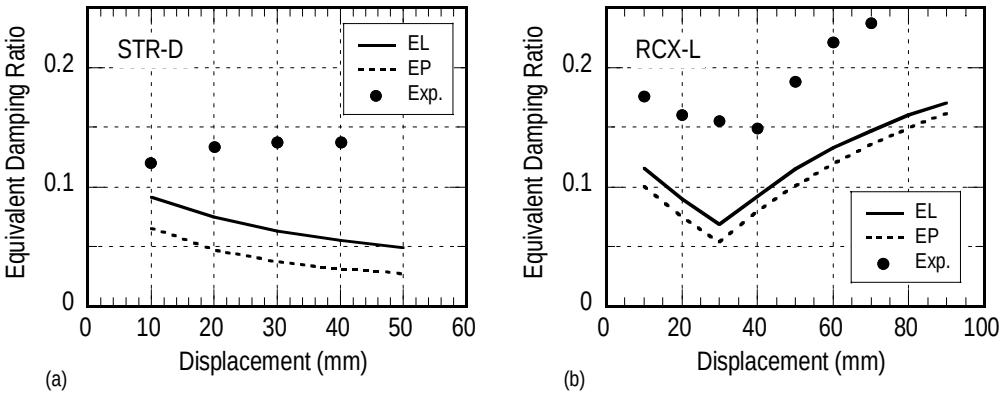

Figure 20. Variations of equivalent damping factor in (a) STR-D, and (b) RCX-L.

interfacial behavior on the damping is about 5% in loose sand cases and 3% in dense sand cases. The underestimation of the equivalent damping is due to ignoring the nonlinearity of the average (volumetric) stress component, depending on the cyclic deformation history in the applied constitutive law for sand, such as variations in the void ratio or dilatancy. The damping characteristics of a structural foundation strongly affect the response of the overall structural system. However, concerning the seismic energy that is input into superstructure, the underestimation of the damping provides a margin of safety when evaluating seismic performance.

Table IV. Variables of parametrical analyses.

Element	Parameters	Range
Soil	Relative Density $D_r(\%)$	55 / 70 / 85
	Initial Earth Pressure Coeff. K_p	0.725 / 2.3 / 4.0
Pile	Reinforcement Ratio $P_w(\%)$	1.27(4-ϕ6)
		2.85(4-ϕ10)
Interface	Element Type	EL / EP

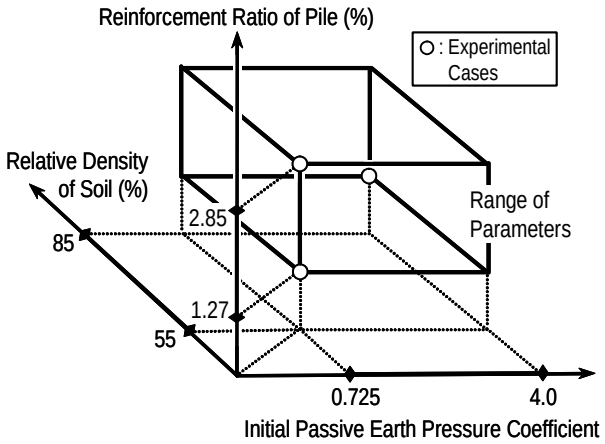

Figure 21. Range of controlling parameters.

4.3. Parametrical investigations of the influence of interfacial behavior on pile response

In order to quantitatively clarify the influence of interfacial behavior, some parametrical analyses were performed in which several soil and pile parameters were varied, as shown in Table IV. The relative density D_r and the initial earth pressure coefficient K_p were selected as the controlling parameters for soil, and the longitudinal reinforcement ratio P_w was chosen as a controlling parameter for the pile. Variations in the relative density D_r affect the shear stiffness of the soil, and the initial earth pressure coefficient K_p is an effective parameter, not only for shear stiffness but also for the stress level at which the pile and the soil separate. The range of each controlling parameter is determined by the experimental conditions shown in Figure 21. These analytical results are accurate to same degree as those in the previous section. Successive examinations were intentionally performed.

Figure 22 shows the maximum damaged depth for all combinations of three parameters and two kinds of interface models, plotted with relative stiffnessK_R. These results show a remarkable effect on the interfacial separation between pile and soil when $P_w = 2.85\%$ but not when $P_w = 1.27\%$. In addition, the higher the relative stiffness K_R is, the larger the maximum damaged depth. However, the relative density D_r does not have such a large

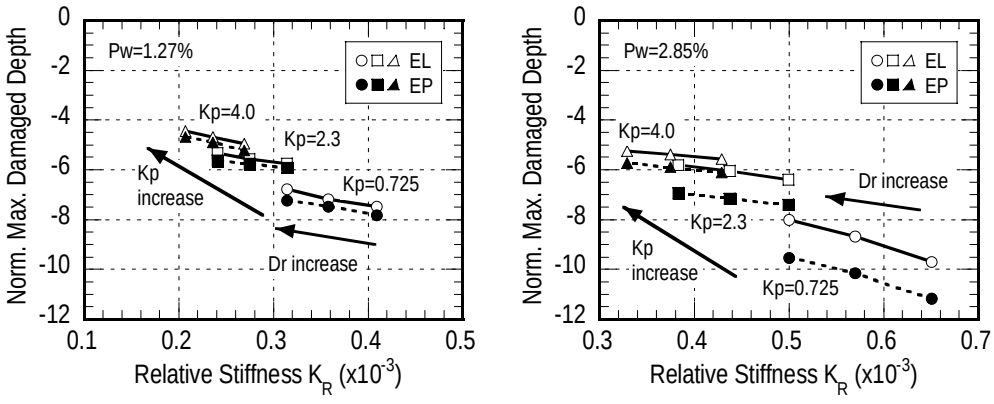

Figure 22. Relationships between maximum damaged depth and relative stiffness; (a) $P_w = 1.27\%$, (b) $P_w = 2.85\%$.

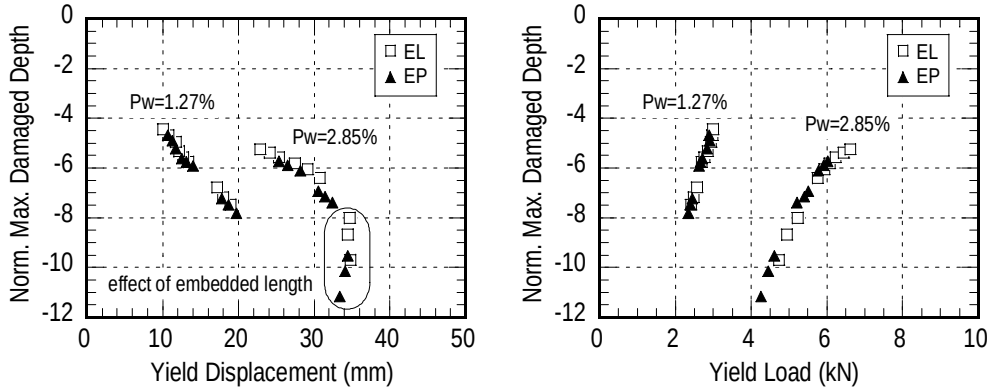

Figure 23. Variations of maximum damaged depth with (a) yield displacement, and (b) yield load.

effect on the depth. In the range of the controlling parameters, the largest difference in the maximum damaged depth is about twice as large as the pile dimension when $K_p = 0.725$ and $P_w = 2.85\%$. These results indicate that the initial earth pressure coefficient is an effective parameter for the maximum damaged depth of a pile. Figure 23 plots the depths for all of the analytical cases together with the yield loads and yield displacements. Both relationships can be linearly approximated in each reinforcement ratio for the pile, independent of the type of model interface element and the soil parameters. This proves that the maximum damaged depth is the important factor that represents the nonlinear interaction between the pile and the soil. The lateral load at the pile head is determined from the depth and the cross section profile of the pile.

5. ANALYTICAL VERIFICATIONS

5.1. Basic concept

The shift to performance-based design of RC structures requires not only developping more precise performance evaluation techniques but evaluating the accuracy of such techniques. The current JSCE seismic design code [2], published in 2002, prescribes the response estimation method for the overall structural system, including the foundation and the surrounding soil, with seismic motion input at the engineering base. When such a method is applied to a structural performance evaluation in the framework of performance-based design, the appropriate partial safety factors should be defined by the level and precision of the response and capacity estimation methods. This chapter discusses some quantitative investigations of the precision of the applied analytical technique that is used to estimate the response of an RC pile-soil system.

An actual pile foundation is subjected to inertial forces from both the surrounding soil and the superstructure. When the inertial force of the superstructure acts on the pile head, the surrounding soil acts as a reaction object. If the analytical method underestimates the transmitted stress level between the pile and the soil and the method is applied to a pile subjected only to the lateral inertial force of the soil, then the sectional force and the deformation of pile will be underestimated. Applying a similar method to a pile subjected only to a lateral force on the pile head due to the response of the superstructure will result in an overestimation of the pile deformation, which comes from the underestimated soil reaction. These two types of analytical errors are canceled in the seismic response analysis of the structural system, indicating that the evaluation of the accuracy of the response estimation under lateral load at the pile head, which is discussed in this chapter, does not coincide with the evaluation of the safety of the structural members or the structural system. In other words, when pile deformation precedes ground deformation (subjected to a lateral inertial force on the pile head), the maximum analytical error margins are included in the estimated value of the response, resulting in the worst possible case of analytical verification.

The evaluation of seismic safety of structures should be based on a seismic response analysis that considers various factors. Note that the evaluation in this chapter does not check seismic performance though analytical verification based on the specific limit states corresponding to the seismic performances prescribed in the JSCE code [2].

5.2. Verification of pile response under the serviceability limit state

In the JSCE code, seismic performance 1, corresponding to the serviceability limit state, is based on the induced stress level caused by a level 1 earthquake. Therefore, the sectional force and deformation of the pile when yielding is reached are factors for analytical verification under the serviceability limit state. The yielding of pile foundation is defined by the three types of limit state: (1) when the sectional moment of the pile reaches the yielding moment; (2) when plastic deformation of surrounding soil is perfectly reached; and (3) when there is vertical deformation of the foundation due to pull-out of the pile from the ground. This section discusses limit state (1) because it relates to the structural performance of pile members.

Figure 24(a) shows the concept of analytical verification under the serviceability limit state. Lateral force $P_{y,cal}$ at the moment the yield moment of pile is reached is assumed to be the static external load P_d, which will be used in subsequent comparisons. This corresponds to

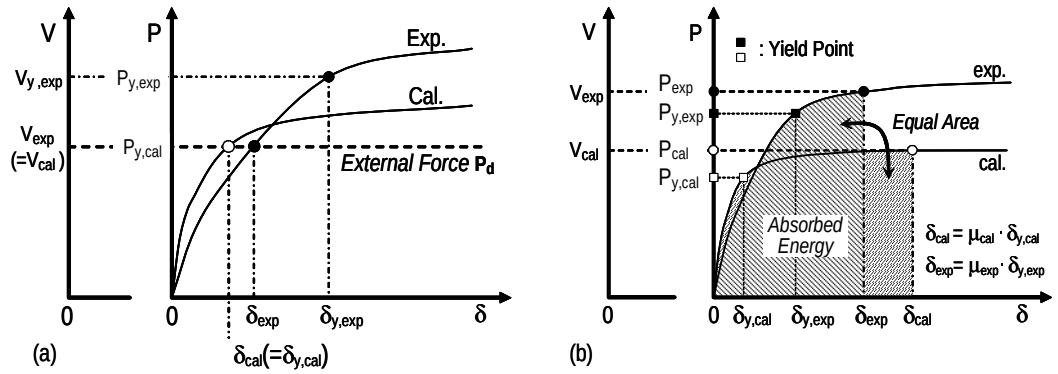

Figure 24. Schematic concept for analytical verifications under (a) serviceablity and (b) ultimate limit states.

the assumption that lateral force P_d acts on the pile head under a level 1 earthquake. Static verifications are performed by comparing the maximum shear force, lateral displacement at the pile head, and maximum tensile strain of the longitudinal reinforcement with the values obtained from the experiment under lateral load P_d. Here, the comparison of the strains of the reinforcement is based on the stress because the longitudinal reinforcement remains elastic. The maximum shear response in the pile is equal to the lateral load on the pile head when it is able to rotate freely. This produces the following equation (3);

$$P_d = V_{cal} = V_{exp} \tag{3}$$

where, V_{cal} is the calculated shear response in the analysis and V_{exp} is the shear response obtained from the experiment.

Therefore, this verification focuses on the response displacement at the pile head and the maximum tensile strain of the longitudinal reinforcement when the pile is subjected to equal shear forces. Table V shows the response displacement ratio R_{d1} calculated by equation (4) and the strain ratio of the longitudinal reinforcement R_{e1} computed by the equation (5).

$$R_{d1} = \delta_{exp}/\delta_{cal} \tag{4}$$

$$R_{e1} = \epsilon_{exp}/\epsilon_{cal} \tag{5}$$

The Model EL that does not include the effect of separation underestimates the response displacement by about 20%, while the Model EP that includes the effect of separation produces estimates that are within 15% of the true value, indicating that the response displacement can be accurately evaluated when the interfacial behavior is incorporated in the analytical model. Both models, but Model EP in particular, overestimate the maximum strain of the longitudinal reinforcement by 10 to 20%, but the experimentally and analytically obtained maximum damaged depths differ. Therefore, in order to achieve stricter verification, the strain distribution in the vertical direction must be considered.

Table V. Verification results for serviceablity limit state.

Factor		Model EL	Model EP
R_{e1}	Range (*average*)	0.83-0.89 (*0.85*)	0.74-0.87 (*0.80*)
	Tendency	**overestimate**	**overestimate**
R_{d1}	Range (*average*)	0.98-1.26 (*1.12*)	0.86-1.12 (*1.01*)
	Tendency	**underestimate**	——

5.3. Verification of pile response under the ultimate limit state

Seismic performance 2 corresponds to the ultimate limit state and is determined by the response displacement (the response ductility ratio) and the residual displacement induced by a level 2 earthquake. However, the pile specimens did not reach the ultimate state in the targeted loading tests and it is impossible to examine the capacity and residual displacement of the piles. Therefore, a simple static verification of the pile response is performed by comparing the absorbed energy of the system to several allowable ductility factors.

Figure 24(b) shows the concept of analytical verification under the ultimate limit state. First, the total absorbed energy E (total area of the cross-hatched zone in Figure 24(b)) is calculated from the analytical result when the allowable ductility ratio μ_a a of the pile is reached. Here, the response displacement δ_{cal} and the shear force V_{cal} at the allowable ductility ratio μ_a a can be obtained from the load and displacement relationship. The above process is based on the assumption that the pile-soil system designed using the allowable ductility ratio μ_a a absorbs the seismic energy E when subjected to a level 2 earthquake. The response displacement δ_{exp} and shear force V_{exp} are then calculated from the results of the experiment when the same energy E is absorbed by the experimental system.

2.0, 3.0, 4.0 and 5.0 were chosen as the allowable ductility ratios for the investigation, and the response displacement and shear force were computed when each allowable ductility ratio is reached. The shear force ratio R_{v2} and displacement ratio R_{d2}, calculated by equations (6) and (7), respectively, are shown in Table VI.

$$R_{v2} = V_{exp}/V_{cal} \tag{6}$$

$$R_{d2} = \delta_{exp}/\delta_{cal} \tag{7}$$

The applied analytical model underestimates by 10 to 30% the response shear force induced in the pile, while the analytical model with nonlinear interface elements tends to produce larger underestimates. However, the degree of the underestimation is relatively small when the allowable ductility ratio is high. On the other hand, the response displacement tends to be overestimated, and the trend appears more conspicuously in the analytical model that has nonlinear interface elements. The response displacement is overestimated by at most 15%.

As stated at the beginning of this section, the simple investigation performed here to verify the analytical model is based only on the load-displacement relationships. Stricter verification that considers the loading history should be carried out after developing a more precise analytical model that includes a detailed material constitutive law for soil.

Table VI. Verification results for ultimate limit state.

Factor	Allowable Ductility μ_a	Range (*average*) Model EL	Model EP
R_{v2}	2.0	1.04-1.32 (*1.19*)	1.21-1.42 (*1.31*)
	3.0	0.98-1.22 (*1.11*)	1.17-1.36 (*1.26*)
	4.0	0.94-1.14 (*1.05*)	1.12-1.33 (*1.22*)
	5.0	0.91-1.09 (*1.00*)	1.08-1.31 (*1.19*)
	Tendency	**underestimate**	**underestimate**
R_{d2}	2.0	0.98-1.08 (*1.02*)	0.92-1.02 (*0.96*)
	3.0	0.93-1.03 (*0.97*)	0.88-0.96 (*0.90*)
	4.0	0.91-1.02 (*0.96*)	0.85-0.94 (*0.88*)
	5.0	0.91-1.03 (*0.96*)	0.83-0.93 (*0.87*)
	Tendency	——	**overestimate**

5.4. Summary

Based on the lateral loading tests of RC piles under ground, numerical simulations using 3D-FEM were carried out using the *dof*-reduced analytical model in which the pile is modeled with beam elements. The influence of the interfacial actions between the pile and the soil on the response behavior of a pile-soil system was investigated. Keeping in mind the application of the proposed method to evaluating actual structural seismic responses, the analytical model was quantitatively verified.

The results of the investigations clearly show that the load-displacement hysteresis at the pile head is highly affected by the difference in the maximum damaged depth, which is produced by interfacial separation in the analytical model. The influence of interfacial separation is more remarkable when the piles have high relative stiffness. However, the restoring force and the displacement are linearly approximated by the maximum damaged depth, and the load-displacement relationship is determined by the depth and the cross sectional profile of the pile, indirectly depending on the soil parameters.

For a damage level equivalent to the seismic performance 1 prescribed in the JSCE code, the analytical model that does not consider interfacial separation slightly underestimates the response displacement and overestimates by 20% the longitudinal reinforcement strain. For a damage level equivalent to seismic performance 2, the model slightly overestimates response displacement and underestimates by 20 to 30% the shear force induced in the pile section. The model that considers interfacial separation produces a higher displacement value and a lower shear force value than the model that does not consider interfacial separation.

6. CONCLUSIONS

This paper describes from the viewpoint of subgrade soil reactions based on the single-layer model an appropriate modeling technique for pile-soil interaction analysis using beam elements. The paper also proposes a basis for developing a guideline for modeling pile-soil systems.

Based on the proposed modeling technique, 3D-FEM simulations of a lateral loading test for RC piles were conducted using *dof*-reduced analytical models, and the influence of the interfacial actions between the pile and the soil on the response behavior of pile-soil systems was investigated. Furthermore, the analytical model was verified quantitatively so that the proposed method can be used to evaluate actual structural seismic responses. The results confirmed that the *dof*-reduced model could produce values within about 30% of the actual values. If the degree-of-freedom of the model is not reduced and the three dimensional effect is included directly in the model, the numerical errors can be further reduced.

The influence of pile behavior on the responses of superstructures and overall systems should be promptly investigated. In this paper, the allowable ductility ratio is used to verify the analytical model regarding a damage level equivalent to seismic performance 2. However, the analytical method requires further verification based on the vertical supporting performance, which is one of the principal requirements of a pile foundation.

ACKNOWLEDGEMENTS

The authors wish to gratefully acknowledge the cooperation of Prof. F. Tatsuoka, Prof. K. Konagai, Assoc. Prof. M. Abe and Assoc. Prof. X. An of the University of Tokyo, and Prof. A. Machida of Saitama University, as well as the cooperation of the members of the structural material laboratory in Saitama University.

REFERENCES

1. JSCE Committee of Civil Engineering of Nuclear Power Facilities. *Seismic Design Manual for Nuclear Electric Power Facilities*. JSCE, 2002.
2. Japan Society of Civil Engineers. *Standard Specification for Design and Construction of Concrete Structures: Seismic Performance Evaluation*. JSCE, 2002.
3. Zhang F, Kimura M, Nakai T, Hoshikawa T. Mechanical behavior of pile foundations subjected to cyclic lateral loading up to the ultimate state. *Soils and Foundations* 2000; **40**(5):1–17.
4. Chai YH, Hutchinson TC. Flexural strength and ductility of extended pile-shafts - II: Experimental study. *Journal of Structural Engineering (ASCE)* 2002; **128**(5):595–602.
5. Maki T, Mutsuyoshi H. Restoring Force and Deformation of Reinforced Concrete Piles. *Journal of Materials, Concrete Structures and Pavements (JSCE)* 2001; **683**(52):103–118. (in Japanese)
6. Maki T, Mutsuyoshi H. Effect of local characteristics between pile and soil on seismic behavior of RC piles under ground. *fib 2003 Symposium on Concrete Structures in Seismic Regions (Proceedings in CD form)*, Athens, Greece, 2003; paper No.140.
7. Maki T, Mutsuyoshi H, Maekawa K. Applicability of fiber model to RC pile-soil interaction analysis. *Journal of Materials, Concrete Structures and Pavements (JSCE)* 2003; **746**(61):57–70. (in Japanese)
8. Maki T, Mutsuyoshi H. Seismic behavior of reinforced concrete piles under ground. *Journal of Advanced Concrete Technology (JCI)* 2004; **2**(1):37–47. (in Japanese)
9. Ishida T, et al. Static and dynamic mechanical properties of materials for model tests (gifu sand) under low confining stress. *Research Report of Electrical Power Center Research Institute* 1981; No.380045:1–36. (in Japanese)
10. Poulos HG. Behavior of laterally loaded piles: I-Single Piles. *Journal of the Soil Mechanics and Foundations Division, Proceedings of ASCE* 1971; **97**(5):711–731.
11. Maki T, Maekawa K, Mutsuyoshi H. Effect of pile modeling on behavior of RC piles under ground. *Proceedings of the Japan Concrete Institute* 2004; **26**(2):1165–1170. (in Japanese)
12. Okamura H, Maekawa K. *Nonlinear Analysis and Constitutive Models of Reinforced Concrete.* Gihodo Shuppan, 1991.
13. Maekawa K, Pimanmas A, Okamura H. *Nonlinear Mechanics of Reinforced Concrete.* Spon Press, New York, USA., 2003.
14. Ohsaki Y. Some notes on Masing's law and non-linear response of soil deposits, *Journal of the Faculty of Engineering, The University of Tokyo (B)* 1980; **35**(4):513–536.

15. An X, Maekawa K, Okamura H. Numerical simulation of size effect in shear strength of RC beams. *Journal of Materials, Concrete Structures and Pavements (JSCE)* 1997; **564**(V-35):297–316.
16. Maki T, Mutsuyoshi H. Study on seismic performance of reinforced concrete piles under ground. *Proceedings of the 3rd International Workshop on Performance-Based Seismic Design and Retrofit of Transportation Facilities (TIT)* 2002; 67–78.